EPJ Web of Conferences **315**, 01024 (2024) https://doi.org/10.1051/epjconf/202431501024
LCWS2024

Reimagining e^+e^- collider precision luminosity measurements

Graham Wilson[1,*] and *Brendon* Madison[1]

[1]Department of Physics and Astronomy, University of Kansas, Lawrence, KS 66045, USA

Abstract. Our recent work has shown that a novel much higher granularity forward calorimetry concept can enable much more detailed and precise reconstruction than the baseline designs based on LEP luminometers, along with the capability of electron/positron/photon separation. This new calorimeter concept is designed primarily to maximize the acceptance for $e^+e^- \to \gamma\gamma$ as an alternative luminosity process, where it serves to define the inner edge of the acceptance (there is no outer edge, as the complete detector is used in the measurement), while continuing to provide the standard luminosity measurement from small-angle Bhabha scattering (SABS). It will also serve as a general forward electromagnetic calorimeter helping ensure hermeticity and detecting individual electrons, positrons, and photons. In this contribution we highlight the Bhabha rejection capability in the context of the $e^+e^- \to \gamma\gamma$ luminosity measurement and motivate the utility of a Bhabha "mini-tracker" consisting of a few planes of upstream thin silicon detectors. This could further refine the e^+/e^- polar angle measurement, aid with charge measurement, improve Bhabha rejection (for $\gamma\gamma$), and, last-but-not-least, help mitigate the beam-induced electromagnetic deflection that biases the Bhabha acceptance by providing high precision longitudinal vertex information in Bhabha events, which can be used to diagnose this effect of the beam on the final-state electron and positron.

1 Introduction

We have been motivated by the requirements on precision luminosity measurement at a future high energy e^+e^- collider detector using both the $e^+e^- \to \gamma\gamma$ process and the standard small-angle Bhabha scattering (SABS) to propose a new approach to the related forward calorimetry. This has focused our attention on how well one can reconstruct high energy electromagnetic showers and in particular those of high energy photons using dedicated electromagnetic calorimeters. The application emphasizes high performance energy, polar angle and azimuthal angle resolutions combined with excellent electron/photon discrimination. A related contribution to this workshop focuses on position/angle resolution [1]. Here, we focus on framing the work in the precision luminosity measurements context with a more substantive discussion of the $e^+e^- \to \gamma\gamma$ process for luminosity, the corresponding requirements and challenges, and an overview of the new forward calorimeter concept.

*e-mail: gwwilson@ku.edu

2 Luminosity measurements at future high energy e^+e^- colliders

Precision luminosity measurement possibilities were reviewed recently as part of the "ECFA Focus topics" exercise [2] highlighting both the established small-angle Bhabha scattering (SABS) based method used to great effect at LEP and the interesting possibility that $e^+e^- \to \gamma\gamma$ can provide a competitive and possibly superior absolute luminosity measurement in the precision regimes of around 10^{-4} targeted/envisaged for future e^+e^- colliders. This work is partly an acceptance of the challenge to explore some of the experimental challenges and limitations of this topic.

3 $e^+e^- \to \gamma\gamma$ process for luminosity

The Born level QED differential cross section for $e^+e^- \to \gamma\gamma$ with possibly longitudinally polarized beams, and with longitudinal polarization values of P_{e^-} and P_{e^+} at high energy, reads as

$$\frac{\mathrm{d}\,\sigma_{\mathrm{Born}}(\mathrm{P_{e^-}},\mathrm{P_{e^+}})}{\mathrm{d}\,\cos\theta_\gamma} = \frac{2\pi\alpha^2}{s}\,(1 - P_{e^-}P_{e^+})\left(\frac{1+\cos^2\theta_\gamma}{\sin^2\theta_\gamma}\right) .$$

The process is well known and a staple of e^+e^- collider measurements such as those at LEP, the highest energy e^+e^- collider to date that operated until the year 2000 [3]. The form of the polarization factor, $(1 - P_{e^-}P_{e^+})$, arises from the equality of the LR and RL cross sections ($A_{\mathrm{LR}} = 0$) and the absence of LL and RR cross sections [4].

The experimentally detectable integrated cross section is obtained by integrating[1] the polar scattering angle from $\cos\theta_\gamma = 0$ to $\cos\theta_\gamma = \cos\theta_\gamma^{\mathrm{min}}$, where $\theta_\gamma^{\mathrm{min}}$ is the minimum detectable photon polar angle. The polarization factor is 1 for unpolarized beams. For the 80% e^- and 30% e^+ baseline polarization for ILC it takes values of either 1.24 for the preferred opposite helicity configurations (LR, RL) used mostly in physics runs or 0.76 for the same helicity configurations (LL, RR) that are assigned some luminosity for measuring the polarization. The cross sections are summarized in Table 1 for $\sqrt{s} = 161$ GeV.

$\theta_\gamma^{\mathrm{min}}$ (°)	$\sigma_{\gamma\gamma}$ (pb)	$\Delta\sigma/\sigma$ (10 μrad)	$\sigma(e^+e^-)/\sigma(\gamma\gamma)$
45	5.3	2.0×10^{-5}	6.1
20	12.7	2.2×10^{-5}	22
15	15.5	2.4×10^{-5}	35
10	19.5	2.9×10^{-5}	68
6	24.6	3.9×10^{-5}	155
2	35.7	8.1×10^{-5}	974

Table 1: Unpolarized $e^+e^- \to \gamma\gamma$ cross-sections at $\sqrt{s} = 161$ GeV for various choices of the angular acceptance cut, $\theta_\gamma^{\mathrm{min}}$. The $\Delta\sigma/\sigma$ column shows the fractional cross section uncertainty when the acceptance edge is understood with an uncertainty of 10 μrad. The last column shows the ratio of Bhabha events to $e^+e^- \to \gamma\gamma$ events for these different acceptance choices for $\sqrt{s} = 161$ GeV. Note that this ratio is much larger for wide angles when the s-channel production is significant (as in $\sqrt{s} \approx m_Z$).

Figure 1 shows the unpolarized Born cross section for different choices of $\theta_\gamma^{\mathrm{min}}$ normalized to that for $\theta_\gamma^{\mathrm{min}} = 20°$, a value representative of the LEP experiments. For $\sqrt{s} = 161$ GeV, the unpolarized Born cross section with $\theta_\gamma^{\mathrm{min}} = 20°$ is 12.7 pb. If the photon acceptance can be

[1] Photon indistinguishability restricts the integration to one hemisphere

extended from 20° down to 35 mrad or below, one can roughly triple the unpolarized cross sections. This would exceed tenfold the unpolarized WW threshold cross section of about 3.5 pb, thus reducing substantially the relative statistical uncertainty from counting $\gamma\gamma$ luminosity events when applied to the measurement of m_{W} as envisaged in [5, 6]. Reducing the substantial Bhabha background when counting $e^+e^- \to \gamma\gamma$ events for luminosity is a challenge in this extended polar angle range. Especially so as the standard tracking acceptance does not extend below about 6° (for ILD [7]).

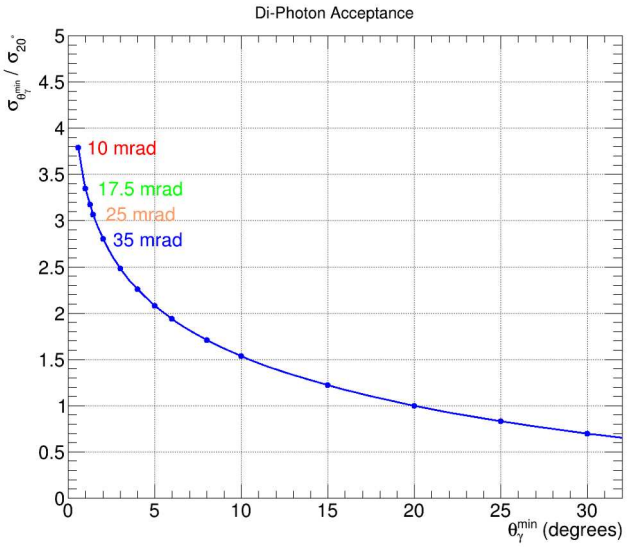

Figure 1: The unpolarized Born cross section for $e^+e^- \to \gamma\gamma$ for different choices of $\theta_\gamma^{\mathrm{min}}$ normalized to $\theta_\gamma^{\mathrm{min}} = 20^\circ$.

A primary advantage of the $e^+e^- \to \gamma\gamma$ process over SABS is the relaxed requirement on knowledge of the detector fiducial acceptance arising from the less steeply varying angular distribution. Our initial approach is to adopt essentially the same type of *inner* acceptance criterion for $e^+e^- \to \gamma\gamma$ as used for SABS (for example the narrow acceptance polar angle exceeding 31.3 mrad used in [8]). This will make for an immense data set of SABS events for constraining the detector response in the region of such an *inner* acceptance cut. For SABS there is also an *outer* acceptance criterion such as polar angle less than 51.6 mrad as used in [8]. Such an outer cut is motivated by reducing electroweak *s*-channel and *s*-*t* interference contributions from the more pure QED *t*-channel contributions to Bhabha scattering. This is basically not needed for $\gamma\gamma$ as the only electroweak contributions enter at loop level. E.g. WW boxes near WW threshold. So the proposal is to have no outer acceptance cut and to use the whole detector. It will likely be necessary to apply an acollinearity cut or similar to the two most energetic photons that would limit the acceptance for multi-photon events; it may nevertheless be possible to retain significant acceptance for $e^+e^- \to \gamma\gamma\gamma$ events with three detected hard photons as was done at LEP.

4 Forward calorimeter concept for precision luminosity

The initial concept for a new forward calorimeter has several features. The key idea is to have a calorimetric tracker rather than a traditional calorimeter and to focus on the precise localization of the initial shower while designing for high precision reconstruction and identification of electrons, positrons, and photons. Initial design features include:

- Precise location of the high-energy photon interaction point (via photon conversion to e^+e^-) in thin absorbers (see Fermi-LAT gamma-ray telescope for extreme version of this [9]).
- High-energy photons need to be longitudinally contained so as to avoid a large constant term as (10, 1, 0.1)% of photons survive for (3, 6, 9) X_0 prior to interaction.
- The goal of unambiguous identification of the photon interaction vertex leads to a design with many thin layers assuming a sampling Si-W ECAL.
- Energy calibration: straightforward with uniform sampling.
- Potential for adoption in part of pixel-based devices. The FoCal prototype achieved 30 μm position resolution for high energy electron showers with ALPIDE sensors [10]. Two planes are adopted in the ALICE-FoCal upgrade.
- Include 0^{th}-layer and maybe more for enhanced e/γ discrimination.
- Emphasize azimuthal measurements for $e^+e^-/\gamma\gamma$ discrimination. Expect about +57 mrad acoplanarity for $B\, z_{LCAL} = 8.7$ Tm at $\sqrt{s} = 91.2$ GeV for forward scattered Bhabhas.
- Particle-by-particle reconstruction capabilities.
- Much more emphasis on energy resolution. Less emphasis on minimal Molière radius.
- Limited solid-angle so cost is not an over-arching concern.
- Retain or exceed performance for Bhabha-based measurement.

These considerations have led us towards concrete design possibilities that emphasize a precision sampling calorimeter. Studies related to evaluating aspects of such a calorimeter design have been carried out using GEANT4 [11] in the following ways:

- Longitudinal segmentation studies based on the `extended/electromagnetic/TestEm3` standard example that keeps track of energy depositions in each detector plane.
- Studies of transverse coordinate reconstruction starting from the `advanced/HGCal_testbeam` example with further refinement of the transverse granularity.
- Related studies of transverse coordinate reconstruction starting from the `advanced/HGCal_testbeam` example where the GEANT4 hits are retained and the energy deposits for arbitrary size candidate cells can be computed.

Results of some of the TestEm3 based studies are shown in Fig. 2 and Fig. 3 indicating that with 10 samples per radiation length an energy resolution of $3.66\%/\sqrt{E}$ can be targeted for photon energies up to 250 GeV, and longitudinal leakage can be avoided by design with a calorimeter of 38 X_0 depth. In these designs the Si thickness, t, is chosen as 750 μm which helps improve the sampling fraction. This is likely to be cost-effective as it reduces the amount of thinning needed for Si crystals; on the other hand it does increase the bias voltage needed for full depletion ($V \sim t^2$).

Initial studies on position resolution were carried out with hexagonal Si cells of area 30 mm^2 with the same longitudinal structure as the CMS HGCAL test-beam configuration used in the GEANT4 `HGCAL_testbeam` example using a test beam type geometry. With a simple energy-weighted center-of-gravity, position resolutions in x and in y of 800 μm

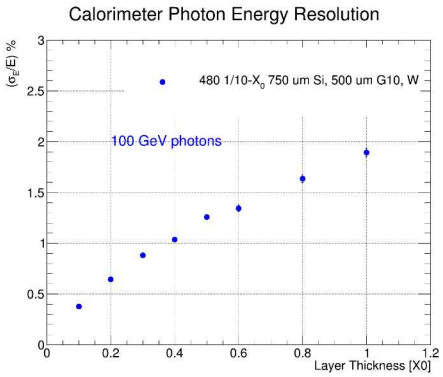

Figure 2: Energy resolutions for 100 GeV photons for design with 0.1 X_0 samples. Results for lower frequency sampling are estimated by layer ganging.

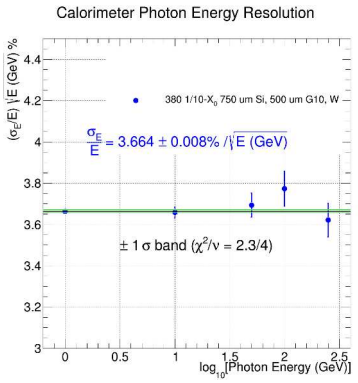

Figure 3: Energy resolution vs photon energy for the first 380 layers of the simulated ECAL indicating no significant leakage and no significant constant term.

were achieved for 100 GeV photons. This was further refined by projecting all the cell energies onto the transverse plane and doing a transverse fit for the incident position using a Grindhammer-Peters like model [12] for the radial profile. Position resolutions in x and in y of 225 μm were achieved for 100 GeV photons. Further study of this algorithm for smaller hexagonal cells - namely of area 1.25 mm^2 led to position resolutions of 112 μm for 100 GeV photons. None of these results exploits yet the initial shower characteristics so we have some confidence that even with rather coarse transverse granularity position resolutions below 100 μm should be readily achievable for photon energies of interest. Studies with GEANT4 hits and arbitrary cell sizes are reported in a separate contribution [1].

5 Bhabha background and rejection potential

For rejecting Bhabha background we have two strategies. Firstly, using tracking and calorimetric information to identify individual electrons preferably using the most upstream detector layers, and secondly event-level information such as the signed acoplanarity associated with the two-particle event. Even if there is no explicit tracking upstream of the chosen calorimeter layout, we can still make the first few layers of the calorimeter relatively transparent and use the presence/absence of measured energy to distinguish electrons from photons.

One of the very attractive features of being able to reconstruct the azimuthal position of photons well is that one can use the difference in reconstructed calorimeter azimuth on each side of the detector to form a signed acoplanarity variable that should be close to zero for $e^+e^- \to \gamma\gamma$. Depending on the detector solenoid field and the net bending power (approximately 8.7 Tm for ILD), the transverse bending caused by the detector solenoid leads to a signed acoplanarity of about +57 mrad for forward-scattered Bhabhas (the vast majority) and a signed acoplanarity of -57 mrad for backward-scattered Bhabhas at $\sqrt{s} = 91.2$ GeV. It is assumed that the B-field is in the electron beam direction, and the signed acoplanarity is defined as

$$\phi^{\mathrm{S}}_{\mathrm{acop}} = [(\phi_{\mathrm{F}} - \phi_{\mathrm{B}}) \bmod 2\pi] - \pi$$

where ϕ_{F} and ϕ_{B} are the azimuths reconstructed from the shower positions in the forward-scattered side (F) and backward-scattered side (B) forward calorimeters. This is illustrated

in Fig. 4 for the small-angle case for running at the Z assuming uncertainties on x and y of 100 μm demonstrating excellent $\gamma\gamma/e^+e^-$ separation.

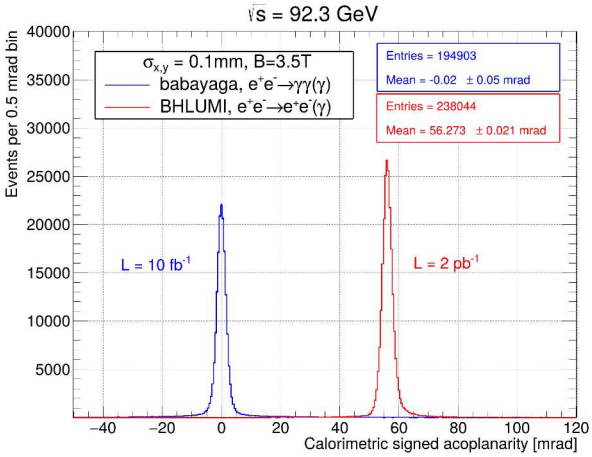

Figure 4: The calorimeter-based signed acoplanarity distributions at $\sqrt{s}$ = 92.3 GeV for small-angle $e^+e^- \to \gamma\gamma$ events generated with babayaga [15] (in blue) and for small-angle Bhabha events generated with BHLUMI [14] (in red) for events with an energetic particle found in the [25, 58] mrad range in each luminometer and satisfying the "isolation cuts" of [8]. The absolute normalization is to an integrated luminosity of 10 fb^{-1} for $\gamma\gamma$ and to 2 pb^{-1} for Bhabhas. Representative calorimetric resolution is taken into account by smearing the (x, y) position of the electromagnetic particles at z = 2.46 m by 100 μm in each transverse direction. The detector solenoid is set to B=3.5T (ILD-like).

Figure 5 shows a similar plot where we try to reproduce the essential experimental criteria of the latest OPAL $e^+e^- \to \gamma\gamma$ paper [13] at LEP2 with a mean $\sqrt{s}$ of 196 GeV, where the angular acceptance cut is set to $|\cos\theta| < 0.93$. Requiring that the acoplanarity be less than 7.5 mrad leads to rejection factors of 171 (for BHWIDE [16] Bhabhas) and 34 (for TEEGG [17] Bhabhas). The latter component consists of essentially (e)eγ events where the detected wide-angle particles are one electron and one photon from predominantly virtual Compton scattering configurations. Such events are troublesome in two ways. Firstly there is only one detected charged particle (to veto) and the acoplanarity values are smaller given that only one of the detected particles bends.

6 Beam-induced electromagnetic deflection studies for SABS

A rather important effect for the luminosity measurement using SABS is the bias in the fiducial acceptance resulting from the electromagnetic deflection of the scattered e^- and e^+ towards the beam axis caused by the electromagnetic forces associated with each produced particle traversing the oppositely charged bunch. This effect was first pointed out in [18] in the context of ILC studies. The effect was recently realized to be important even in the LEP context resulting in a significant correction to the inferred number of light neutrinos coupling to the Z [19]: for the benchmark leading-order Bhabha case with inner and outer scattering angles of 31.3 and 51.6 mrad, the net effect at LEP is estimated to be a bias in the SABS luminosity estimate of -0.1059% at $\sqrt{s}$ = 91.2 GeV. The size of the effect depends on details

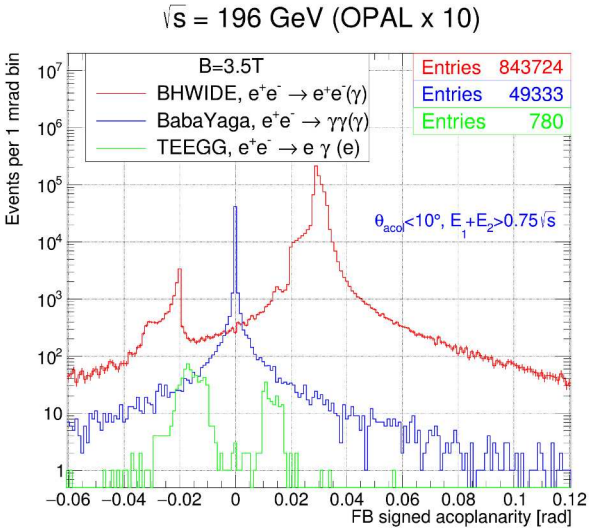

Figure 5: The signed acoplanarity distributions at $\sqrt{s} = 196$ GeV for Bhabha events using the BHWIDE event generator v1.05 (red), for radiative t-channel Bhabha events using the TEEGG event generator v7.2 (green) and compared with that for $e^+e^- \to \gamma\gamma$ events generated with babayaga (blue). All simulations are normalized to an integrated luminosity of 6.72 fb^{-1} and reflect a polar angle requirement of $|\cos\theta| < 0.93$ to emulate the OPAL analysis. The detector solenoid is set to B=3.5T (ILD-like) and the luminosity calorimeter is located at $z = 2.46$ m.

of the accelerator design including bunch populations and beam sizes and is expected to decrease with higher beam energy (less electromagnetic deflection) as already shown in [18]. For ILC operating at the Z, the luminosity bias estimate in the studies from 2007 were found to be in the 1–2% range. This suggests that precision goals at the Z at the 10^{-4} level or better level using SABS will depend on how well these beam effects on the outgoing electron and positron acceptance can be controlled.

We have recently reproduced these effects using Guinea-PIG [20] for LEP running at the Z ($\sqrt{s} = 91.2$ GeV) following the procedure outlined in [19] where nominal lowest-order Bhabha events are scattered at either 31.3 mrad or 51.6 mrad in the center-of-mass and the outgoing Bhabha particles are tracked through the electromagnetic field of the opposing bunch after accounting for the motion of the colliding electron and positron. We find a nominal luminosity bias of $-0.1059 \pm 0.0001\%$ assuming a θ^{-3} distribution in excellent agreement with the -0.1059% computed in [19]. On the other hand the average inner/outer deflections are 13.02 ± 0.01 μrad / 11.42 ± 0.01 μrad, disagreeing with the 12.81/11.19 μrad values computed previously. It is known that some differences can result from different computational parameters (grid size). Applying this procedure to the latest beam parameters for ILC Z running [21] at $\sqrt{s} = 91.2$ GeV leads to the inner/outer electron being deflected by on average 146.87 ± 0.04 μrad / 105.10 ± 0.03 μrad resulting in a luminosity bias of $-1.248 \pm 0.001\%$.

Some strategies to address this may be to exploit asymmetries in the response expected as a function of the scattering azimuth (Fig. 6) and as a function of the longitudinal vertex position as seen in Fig. 7 to produce suitable diagnostic measurements. The azimuthal angle can be easily measured and there is some modulation of the outer deflection angle with azimuth (about 1.5 μrad), but the inner deflection angle appears to show no significant azimuthal de-

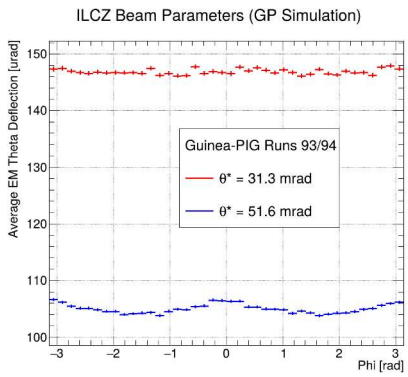

Figure 6: Average EM deflection vs azimuth for the two scattering angles for the ILC Z configuration.

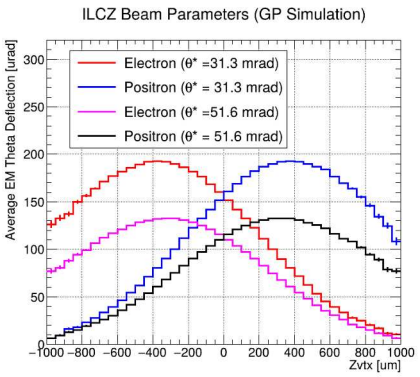

Figure 7: Average EM deflection vs longitudinal vertex position (in microns) for the two scattering angles and for each final-state particle charge for the ILC Z configuration.

pendence. The longitudinal vertex distributions are at first sight much more promising showing large variations of average electromagnetic deflection on longitudinal vertex position, but the ability to measure $z_{\rm vtx}$ for very far forward scattered electrons is much more difficult given that the ILC luminous region at the Z has an rms spread of only 290 μm. It remains to be seen how well a forward calorimeter can be equipped to measure the longitudinal vertex.

There are potentially ways to mitigate the size of the effect by for example reducing the SABS acceptance or by adjusting the event selection requirements. Nevertheless if the goal is to achieve 10^{-4} absolute luminosity precision at the Z one will likely need to understand these corrections that result from details of the actual beam parameters at at least a level of one part in 100. This appears daunting unless there can be useful experimental diagnostics like the longitudinal vertex asymmetries suggested in [19] that can only be enabled if the $z_{\rm vtx}$ resolution is commensurate with the beam-spot length.

7 Conclusions

We report on studies associated with designing a new approach to precision luminosity with a precision sampling calorimeter that potentially could reach below $4\%/\sqrt{E}$ in energy resolution, would provide superb azimuthal resolution helping enable the use of the $e^+e^- \to \gamma\gamma$ QED process for luminosity including within the usual luminosity calorimeter acceptance, and would have excellent polar angle resolution and electron rejection using more of a tracking approach. It seems prudent to plan on supplementing the usual precision luminosity approach of small-angle Bhabha scattering with the use of $e^+e^- \to \gamma\gamma$ given that the $\gamma\gamma$ process avoids the problematic EM deflection issue for Bhabhas, has intrinsically less challenging polar-angle metrology requirements than Bhabhas, and has some theoretical advantages. We emphasize that the design of the luminosity calorimetry is not set in stone by design ideas developed in the early 90's - rather it is a topic where the increased requirements considered today can lead to distinct advantages and opportunities in the detector design and the related overall physics potential.

8 Acknowledgements

This work is partially supported by the US National Science Foundation (NSF) under awards NSF 2013007 and NSF 2310030 and benefited from use of the HPC facilities operated by the Center for Research Computing at the University of Kansas supported in part through the NSF MRI Award 2117449.

References

[1] B. Madison and G. Wilson, "Novel position reconstruction methods for highly granular electromagnetic calorimeters", these proceedings (2024).

[2] J. de Blas *et al.* "Focus topics for the ECFA study on Higgs/Top/EW factories", [arXiv:2401.07564 [hep-ph]].

[3] S. Schael *et al.* [ALEPH, DELPHI, L3, OPAL and LEP Electroweak], "Electroweak Measurements in Electron-Positron Collisions at W-Boson-Pair Energies at LEP," Phys. Rept. **532**, 119-244 (2013) doi:10.1016/j.physrep.2013.07.004 [arXiv:1302.3415 [hep-ex]].

[4] G. Moortgat-Pick *et al.*, "The role of polarized positrons and electrons in revealing fundamental interactions at the linear collider", Phys. Rept. **460**, 131-243 (2008) [arXiv:hep-ph/0507011 [hep-ph]].

[5] G. W. Wilson, "Updated Study of a Precision Measurement of the W Mass from a Threshold Scan Using Polarized e^- and e^+ at ILC," [arXiv:1603.06016 [hep-ex]].

[6] P. Azzurri, "The W mass and width measurement challenge at FCC-ee," Eur. Phys. J. Plus **136**, (2021) 1203. [arXiv:2107.04444 [hep-ex]].

[7] H. Abramowicz *et al.*, "International Large Detector: Interim Design Report", (2020) https://doi.org/10.48550/arXiv.2003.01116

[8] G.Abbiendi *et al.*, [OPAL Collab.] "Precision Luminosity for Z^0 Lineshape Measurements with a Silicon-Tungsten Calorimeter", Eur. Phys. J. C (2000) 373. https://doi.org/10.1007/s100520000353

[9] W. B. Atwood *et al.*, "Design and Initial Tests of the Tracker-Converter of the Gamma-ray Large Area Space Telescope," Astropart. Phys. **28** (2007), 422-434 doi:10.1016/j.astropartphys.2007.08.010

[10] A. P. de Haas *et al.*, "The FoCal prototype—an extremely fine-grained electromagnetic calorimeter using CMOS pixel sensors," JINST **13** (2018) no.01, P01014 doi:10.1088/1748-0221/13/01/P01014 [arXiv:1708.05164 [physics.ins-det]].

[11] S. Agostinelli *et al.* [GEANT4], Nucl. Instrum. Meth. A **506** (2003), 250-303 doi:10.1016/S0168-9002(03)01368-8

[12] G. Grindhammer and S. Peters, "The Parameterized Simulation of Electromagnetic Showers in Homogeneous and Sampling Calorimeters", Proceedings of Int. Conf. on Monte Carlo Simulation in High Energy and Nuclear Physics, Tallahassee, Florida, USA, (1993) https://doi.org/10.48550/arXiv.hep-ex/0001020

[13] G. Abbiendi *et al.*, [OPAL Collab.], "Multiphoton production in e^+e^- collisions at $\sqrt{s}$ = 181–209 GeV," Eur. Phys. J. C **26** (2003), 331-344 doi:10.1140/epjc/s2002-01074-5 [arXiv:hep-ex/0210016 [hep-ex]].

[14] S. Jadach, W. Placzek, E. Richter-Was, B. F. L. Ward, and Z. Was, "Upgrade of the Monte Carlo program BHLUMI for Bhabha scattering at low angles to version 4.04," Comput. Phys. Commun. **102** (1997), 229-251 doi:10.1016/S0010-4655(96)00156-7

[15] G. Balossini, C. Bignamini, C. M. C. Calame, G. Montagna, O. Nicrosini, and F. Piccinini, "Photon pair production at flavour factories with per mille accuracy," Phys. Lett. B **663** (2008), 209-213 doi:10.1016/j.physletb.2008.04.007 [arXiv:0801.3360 [hep-ph]].

[16] S. Jadach, W. Placzek, and B. F. L. Ward, "BHWIDE 1.00: O(alpha) YFS exponentiated Monte Carlo for Bhabha scattering at wide angles for LEP-1 / SLC and LEP-2," Phys. Lett. B **390** (1997), 298. [arXiv:hep-ph/9608412 [hep-ph]].

[17] D. Karlen, "Radiative Bhabha Scattering for Singly Tagged and Untagged Configurations," Nucl. Phys. B **289** (1987), 23-35 doi:10.1016/0550-3213(87)90369-5

[18] C. Rimbault, P. Bambade, K. Monig, and D. Schulte, "Impact of beam-beam effects on precision luminosity measurements at the ILC," JINST **2**, P09001 (2007) doi:10.1088/1748-0221/2/09/P09001

[19] G. Voutsinas, E. Perez, M. Dam, and P. Janot, "Beam-beam effects on the luminosity measurement at LEP and the number of light neutrino species," Phys. Lett. B **800** (2020), 135068 doi:10.1016/j.physletb.2019.135068 [arXiv:1908.01704 [hep-ex]].

[20] D. Schulte, "Study of Electromagnetic and Hadronic Background in the Interaction Region of the TESLA Collider,", Ph.D. Thesis, University of Hamburg (1996), DESY-TESLA-97-08.

[21] K. Yokoya, K. Kubo, and T. Okugi, "Operation of ILC250 at the Z-pole," [arXiv:1908.08212 [physics.acc-ph]].